ACKNOWLEDGMENT

Acknowledgment is made to the Donors of the Petroleum Research Fund administered by the American Chemical Society, for the partial support of this research. Also thanks are due to Pittsburgh Activated Carbon Division of the Calgon Corporation for supplying the carbon particles.

NOTATION

a_b = surface area of bubbles per unit volume of bubbles, cm^{-1}

a_s = outer surface area of particles per unit volume of particles, cm^{-1}

C_g = concentration in gas; C_{gi} and C_{go} refer to inlet and outlet streams, respectively; $mole/cm^3$

C_L = concentration in liquid; C^* is concentration in equilibrium with C_g; $mole/cm^3$ (For sulfuric acid g-equiv./cm^3)

d_p = particle diameter (assumed to be spherical), cm

F = total volumetric flow rate of gas, cm^3/s

H = ratio of equilibrium concentration in gas phase to that in liquid phase ($H = C_g/C^*$)

K = adsorption constant for linear isotherm ($\rho_p q = K C_L$)

k'_{Ad} = adsorption rate constant for oxygen, defined by Equation (17), s^{-1}

k_L = mass transfer coefficient from gas bubble interface to bulk liquid, cm/s

k_r' = apparent reaction rate constant defined by Equation (13); includes effects of mass transport resistances, s^{-1}

k_r = intrinsic rate constant at catalyst site, s^{-1}

k_s = mass transfer coefficient from liquid to particle, cm/s

L = total height of slurry above entrance of gas bubbles, cm

M_s = mass of liquid-free particles in slurry, g

m = fraction solids in slurry, $M_s/V_L\rho_L$

q = adsorbed concentration, mole/(g of carbon particles)

r_{Ad} = total adsorption rate of oxygen, mole/s

r_{O_2} = total reaction rate of oxygen; r_{SO_2} is rate for sulfur dioxide, mole/s

t = time, s

V_b = total volume of bubbles in slurry, cm^3

V_L = total volume of particle- and bubble-free liquid in slurry, cm^3

z = vertical distance measured from entrance of gas bubbles into slurry, cm

Greek Letters

α = parameter defined by Equation (2), cm^{-1}

ρ_L = density of particle-free and bubble-free liquid in slurry, g/cm^3

ρ_p = density of liquid-free particles, g/cm^3

ϵ_p = porosity of particles

LITERATURE CITED

Bates, S. J., and W. P. Baxter, *International Critical Tables*, **5**, 12 (1929).

Furusawa, T., and J. M. Smith, "Fluid-Particle and Intra-Particle Mass Transport Rates in Slurries," *Ind. Eng. Chem. Fundamentals*, **12**, 197 (1973).

Happel, J., M. A. Hnatow, and A. Rodriguez, "Use of Tracers in Study of Catalytic Oxidation of Sulfur Dioxide," *AIChE J.*, **19**, 1075 (1973).

Hartman, M., J. R. Polek, and R. W. Coughlin, "Removal of Sulfur Dioxide from Flue Gas by Sorption and Catalytic Reaction on Carbon," *Chem. Eng. Progr. Symp. Ser. No. 115*, **67**, 7 (1971).

Hartman, M., and R. W. Coughlin, "Oxidation of SO_2 in a Trickle-bed Reactor with Carbon," *Chem. Eng. Sci.*, **27**, 867 (1972).

Joyce, R. S., R. T. Lynch, R. F. Sutt, and G. S. Tobias, "Effective Recovery of Dilute SO_2," Third Joint Meeting of the Am. Inst. Chem. Engrs. and Inst. Mex. de Ing. Quimicos, (Denver) (1970).

Juvekar, V. A., and M. M. Sharma, "Adsorption of CO_2 in a Suspension of Lime," *Chem. Eng. Sci.*, **28**, 825 (1973).

Misic, D. M., and J. M. Smith, "Adsorption of Benzene in Carbon Slurries", *Ind. Eng. Chem. Fundamentals*, **10**, 380 (1971).

Otake, T., S. Tone, Y. Yokota, and K. Yoshirmura, "Kinetics of Sulfur Dioxide Oxidation over Activated Carbon," *J. Chem. Eng. Japan*, **4**, 155 (1971).

Rabe, A. E., and J. F. Harris, "Vapor Liquid Equilibrium Data for the Binary System, Sulfur Dioxide and Water," *J. Chem. Eng. Data*, **8**, 333 (1963).

Seaburn, J. T., and A. J. Engel, "Sorption of Sulfur Dioxide by Suspension of Activated Carbon in Water," *AIChE Symp. Ser. No. 134*, **69**, 71 (1973).

Siedlewski, Y. U., "The Mechanism of Catalytic Oxidation on Activated Carbon, The Role of Free Carbon Radicals in the Oxidation of SO_2 to SO_3," *Intern. Chem. Eng.*, **5**, 608 (1965).

Siemes, W., and W. Weiss, "Mixing of Liquids by Means of Gas Bubbles in Narrow Columns," *Chem. Ing. Tech.*, **29**, 727 (1957).

Smith, D. F., *International Critical Tables*, **3**, 271 (1929).

Part II. Mass Transfer Studies

Bubble-to-liquid, liquid-to-particle, and intraparticle mass transport effects were all found to be significant for some conditions in a three-phase slurry reactor operated for the oxidation of SO_2 at 25°C and 1 atm. In particular, intraparticle diffusion was important for particles as small as 99 microns (effectiveness factor = 0.45).

Effective diffusivities determined from reaction, desorption, and adsorption data for O_2, H_2SO_4, and SO_2 indicated that surface diffusion was appreciable for SO_2 but not for oxygen. These results are consistent with the kinetic results in Part I which suggested that the rate-controlling step was a chemisorption process for oxygen on the pore surface of the carbon particles.

SCOPE

Three-phase slurry reactors have the advantages of more uniform temperature and lower intraparticle resistances in comparison with reactors employing larger catalyst particles, for example, trickle-bed systems. Nevertheless, several transport effects can significantly affect the observed reaction rate in slurries. Gas bubble-to-liquid transport can be important and may be estimated using k_L data reported, for example, by Sherwood and Farkas (1966), Misic and Smith (1971) and Juvekar and Sharma (1973). Liquid-to-particle rate coefficients k_s are also available (Prasher and Wills, 1973; Levins and Glastonburg, 1972; Furusawa and Smith, 1973; Brian et al., 1969).

The potential significance of intraparticle diffusion in slurries has been overlooked until recently, possibly because the particles in such reactors are comparatively small. However, the diffusivity in liquid-filled pores is also much smaller than in gaseous systems. Recent results (Hartman and Coughlin, 1972, see Part I; Furusawa and Smith, 1973; Komiyama and Smith, 1974a) have shown that effectiveness factors can be much less than unity for liquid-filled pores in particles of about 100 microns.

This second part of the study of the oxidation of SO_2 in aqueous slurries of carbon particles was undertaken to evaluate the importance of all of these mass transfer resistances. Of particular interest was the significance of intraparticle diffusion and the relation between the intraparticle transport properties of O_2, SO_2, and H_2SO_4 and the kinetics found in Part I.

CONCLUSIONS AND SIGNIFICANCE

The three mass transfer resistances in a three-phase slurry reactor were evaluated from reaction data by varying the concentration of catalyst particles and the particle size. The bubble-to-liquid coefficient k_L agreed reasonably well with data in the literature. The liquid-to-particle rate coefficient k_s was determined for each particle size. The results showed that the correlation of Brian et al. (1969) in terms of the energy dissipation rate could be used to predict k_s values in the slurry reactor with satisfactory accuracy. Both of these resistances affected the measured rate importantly at low concentrations of particles in the slurry and for large particles.

The effects of intraparticle diffusion were most significant; effectiveness factor was 0.45 for 99-micron particles and only 0.021 for particles 2.59 mm in diameter. Even for particles whose d_p averaged 30 microns, the combined effect of liquid-to-particle and intraparticle resistances was about 20%, with intraparticle diffusion accounting for 75% of the total. In view of such results, observed rates for SO_2 oxidation on various kinds of activated carbons are not indicative of intrinsic activity unless the particle sizes are identical. This situation was illustrated by analysis of observed rate data of Seaburn and Engel (1973) for eight different carbons.

Analysis of the transport properties for the individual components indicated that surface diffusion was of equal importance with pore volume diffusion for SO_2. The activated carbon had a high adsorption capacity for SO_2. From this and the very high adsorption rate it was concluded that physical adsorption was involved. The effective diffusivities determined for both oxygen and H_2SO_4 indicated insignificant surface transport. These data gave a pore-volume tortuosity factor of about 3.2 for PAC particles. Such results are consistent with the chemisorption of oxygen being the controlling step in the reaction, as concluded in Part I.

The reaction

$$SO_2(g) + 1/2\,O_2(g) + H_2O(l) \rightarrow H_2SO_4(aq.) \quad (1)$$

provides an attractive medium for studying mass transfer effects in a three-phase aqueous slurry reactor using activated carbon particles as the catalyst. The rate was found (Part I) to be first order in the concentration of oxygen in the liquid phase and zero order with respect to sulfur dioxide. With a large excess in the feed gas, the concentration of oxygen is nearly constant, even for large SO_2 conversions. Since the solubility of oxygen is much lower than that for sulfur dioxide, oxygen is the limiting reactant. The low solubility of oxygen means that the gas bubble-to-liquid resistance is determined by the bubble interface-to-liquid rate coefficient k_L (Calderbank, 1959). In a well-mixed slurry the mass transfer resistance in the bulk liquid is negligible. This leaves three potentially significant transport effects: (1) bubble interface-to-liquid (k_L), (2) liquid-to-particle (k_s), and (3) intraparticle diffusion in the liquid-filled pores (D_e). In terms of oxygen concentrations, the rate at steady state may be expressed in three ways:

$$r_{O_2} = k_L\, a_b\, V_b\, (C^* - C_L)$$

$$= k_s\, a_s \left(\frac{M_s}{\rho_p}\right)(C_L - C_s) = k_r\, E_f \left(\frac{M_s}{\rho_p}\right) C_s \quad (2)$$

The rate of reaction on the carbon particles is given in terms of the effectiveness factor E_f and the first-order kinetics found in Part I; C^* is the oxygen concentration in the liquid in equilibrium with the gas, according to the expression

$$C^* = C_g/H \quad (3)$$

The data reported here were obtained at 25°C. At this temperature $H = 35.4$ (Loomis, 1929).

The rates of reaction r_{O_2} were calculated from the measured concentrations of sulfur dioxide using Equation (12) of Part I. Then an apparent rate constant k'_{rm} was obtained from r_{O_2}, C^* and the expression

$$r_{O_2} = k'_{rm}\, C^* \left(\frac{M_s}{\rho_p}\right) \quad (4)$$

The individual coefficients k_L, k_s, and $E_f k_r$ can be expressed in terms of the rate by eliminating the concentrations from Equations (2), giving

$$\frac{C^*}{r_{O_2}} = \frac{1}{k_L\, a_b\, V_b} + \frac{\rho_p}{M_s}\left(\frac{1}{k_s\, a_s} + \frac{1}{k_r\, E_f}\right) \quad (5)$$

Using Equation (4), the individual coefficients are related to the overall rate constant k'_{rm} by the relation

$$\frac{1}{k'_{rm}} = \frac{M_s}{\rho_p\, a_b\, V_b\, k_L} + \frac{1}{k_s\, a_s} + \frac{1}{k_r\, E_f} \quad (6)$$

TABLE 1. SCOPE OF REACTION MEASUREMENTS

Particle diameter[a], mm = 0.030 to 2.59
Volume of liquid (pure water), V_L cm^3 = 900
Mass of solids, M_s, g = 1.25 to 42.4
Inlet gas concentration[b], %: SO_2 = 1.2 to 2.3; O_2 = 21
Total gas flow rate, cm^3/min. = 2000 (at 25°C, 1 atm)
Impeller speed, rev./min. = 550 ~ 650

[a] The particle sizes are arithmetic averages of the following ranges (all values in mm): d_p = 0.03; 0 to 0.061. d_p = 0.099; 0.074 to 0.124. d_p = 0.542; 0.495 to 0.589. d_p = 1.05; 0.99 to 1.11. d_p = 2.59; 2.38 to 2.80.
[b] Helium made up the remainder of the gas mixture.

Rate measurements were made to evaluate separately k_L, k_s, E_f, and k_r using Equations (5) or (6). The data were measured at 25°C and atmospheric pressure using the apparatus (Pyrex vessel) and procedures described in Part I. Major variables were M_s and particle size. Due to the high heat capacity of the slurry liquid with respect to the heat of reaction, the system operated isothermally. The range of variables is given in Table 1. The properties of PAC particles were listed in Table 1 of Part I. The inlet gas stream contained 21% oxygen, a large excess, so that the concentration of oxygen was essentially constant for all the data.

BUBBLE-TO-LIQUID MASS TRANSFER (k_L)

Rate values were obtained for two particle sizes [$(d_p)_{ave}$ = 0.030 or 0.099 mm] and for several concentrations of particles in the slurry. Since the intrinsic rate is zero order in SO_2 and the oxygen concentration is constant, the rate results for a given particle size are, according to Equation (5), a function only of M_s. Hence, a plot of $1/r_{O_2}$ vs. $1/M_s$ should be linear, as originally suggested by Sherwood and Farkas (1966). Figure 1 shows that the lines for the two particle sizes have the same intercept indicating that k_L was not affected by the particle size. From the intercept and C^* [calculated from Equation (3)]

$$k_L\, a_b\, V_b = 97.\ \text{cm}^3/\text{s} \qquad (7)$$

Knowledge of this product is sufficient to evaluate the remaining mass transfer resistances; k_L is not required. However, an approximate value was determined. From the increase in level when gas was bubbled through the agitated slurry, V_b was 63 cm^3. Hence $k_L\, a_b$ = 1.54 s^{-1}. The bubble diameter using the fritted disk (described in Part I) was estimated to be 3 mm. This estimation was made by visually comparing the bubbles in our system with those in the Misic and Smith's (1971) apparatus. In the latter work the bubble diameter was determined photographically to be 1.8 mm. With this bubble size a_b = 20 cm^{-1}, assuming spherical bubbles, and k_L was 7.7 × 10^{-2} cm/s.

Using a vessel of similar geometry to that for our work, Juvekar and Sharma (1973) showed that k_L was independent of impeller speed in the range 1000 to 2000 rev./min. Assuming that this nondependency holds down to 550 to 650 rev./min (Table 1), their correlation gives 8.0 × 10^{-2} cm/s for our system. With the impeller and vessel (described in Part I) used in our work, the energy dissipation rate is known (Furusawa and Smith, 1973) to be about 2.4 × 10^4 ergs/(s)(g of liquid). For this energy dissipation rate an extension of the correlation of Prasher and Wills (1973) gives 1.2 × 10^{-1} cm/s. However, the correlation was proposed for energy rates up to only 4.3 × 10^3 erg/(s)(g). The value of Misic and Smith (1971) for benzene absorption in a stirred gas-washing bottle of water was 4 × 10^{-2} cm/s.

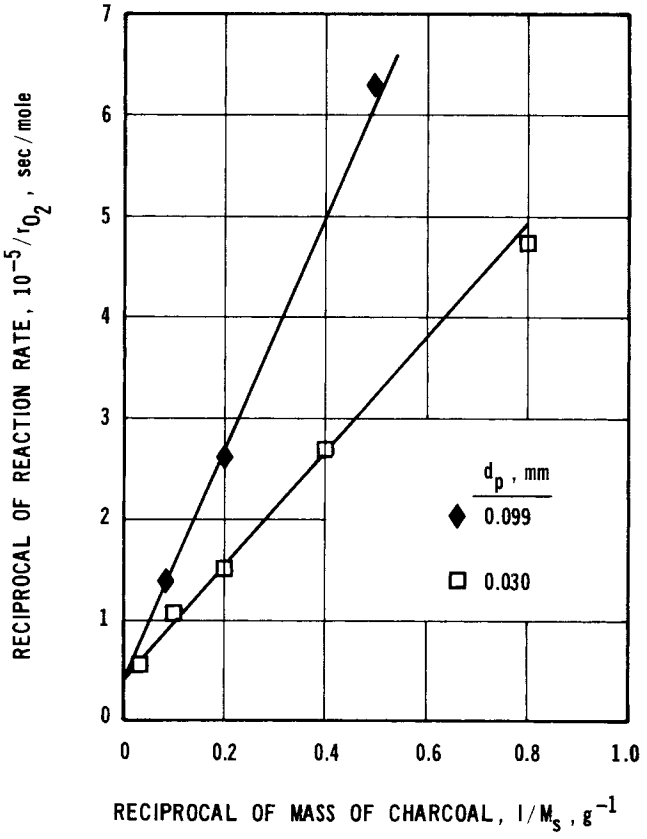

Fig. 1. Reaction rate vs. particle concentration.

LIQUID-TO-PARTICLE MASS TRANSFER (k_s)

The resistance to mass transfer between particles and fluid in the slurry was determined by comparing the slurry results with those when the particles were contained in baskets made of stainless steel screen. The baskets were held stationary in a frame placed inside the Pyrex vessel. For the two largest particles four baskets of 20 mesh screen (15 × 25 mm cross section, 55 mm in height) were located vertically at equal distances around the inner circumference of the vessel. For the smallest particles eight baskets of 40 mesh screen (10 × 10 mm cross section, 20 mm in height) were used. The arrangement of the baskets and frame in the vessel is described in earlier work (Komiyama and Smith, 1974a) where the same procedure was used to eliminate particle-to-fluid transport resistance. Since the finest screen that would allow free passage of liquid and yet contain the particles was about 40 mesh, this method could be used only for the three largest particle sizes (0.542, 1.05, and 2.59 mm).

For the data with particles held in the stationary baskets, $k_s\, a_s$ becomes very large so that Equation (6) reduces to

$$\frac{1}{k'_{rmb}} = \frac{M_s}{\rho_p\, a_b\, V_b\, k_L} + \frac{1}{k_r\, E_f} \qquad (8)$$

Subtracting Equation (8) from Equation (6) gives

$$\frac{1}{k_s\, a_s} = \frac{1}{k'_{rm}} - \frac{1}{k'_{rmb}} \qquad (9)$$

The values of k'_{rm} and k'_{rmb} obtained from the data and Equation (4) are shown in Figure 2 and in the 3rd and 4th columns of Table 2. The corresponding mass transfer coefficients k_s calculated from Equation (9) are listed as experimental values in the fifth column of Table 2. The

TABLE 2. RATE CONSTANTS AND EFFECTIVENESS FACTORS FOR OXYGEN

d_p, mm	$k_L a_b$, s^{-1}	Measured rate constant, s^{-1} k'_{rm}	k'_{rmb}	k_s, cm/s Experimental	Predicted	$k_r E_f$, s^{-1}	E_f Experimental[b]	Estimated[c]
0.030	1.54[a]	5.20			0.0587	5.68	0.861	0.850
0.099	1.54[a]	2.46			0.0348	3.08	0.451	0.447
0.542	1.54[a]	0.500	0.602	0.0267	0.0255	0.645	0.0978	0.0967
1.05	1.54[a]	0.217	0.287	0.0203	0.0243	0.301	0.0456	0.0515
2.59	1.54[a]	0.112	0.133	0.0308	0.0242	0.143	0.0217	0.0209

[a] For 0.03 and 0.099 mm particles, $k_L a_b V_b$, and hence $k_L a_b$, was found to be the same (same intercept in Figure 1). The values of $k_L a_b$ for the larger particle sizes are assumed also to be independent of particle size.

[b] $k_r E_f/6.6$.

[c] $M = \frac{d_p}{2}\sqrt{\frac{6.6}{5.35 \times 10^{-6}}}$ was used for the relation between E_f and M.

area per unit volume a_s was calculated by assuming that the particles were spherical.

The correlations of Brian et al. (1969) and Furusawa and Smith (1973) may be used to predict k_s from a special particle Reynolds number, although no gas bubbles were present in the data upon which these correlations were based. The energy dissipation rate ϵ, per unit mass of slurry liquid, is necessary. This may be calculated from the power consumption P and the impeller speed using the following equations (Furusawa and Smith, 1973):

$$\epsilon = \frac{P}{W} = \frac{N_p \rho_L N^3 d_I^5 \phi}{W} \tag{10}$$

where the power number N_p is defined

$$N_p = \frac{P}{\rho_L N^3 d_I^5} \tag{11}$$

and ϕ is a correction for the effect of gas bubbles on the energy consumption. N_p has a value of 9.5 for the particular geometry of the impeller and reactor system used in our work. For the conditions of the present study, $F/N\ d_I^3 < 0.035$, Calderbank (1958) gives ϕ as

$$\phi = 1 - 12.6\ \frac{F}{N\ d_I^3} \tag{12}$$

At $N = 600$ rev./min. and $W = 900$ g, ϵ from Equations (10) and (12) was 2.43×10^4 erg/(s)(g); ϕ was 0.67. This value of ϵ and the viscosity of the liquid determines the type of Reynolds number to use for predicting k_s. The energy dissipation rate is related to an eddy size η

$$\eta = \left(\frac{\nu^3}{\epsilon}\right)^{1/4} \tag{13}$$

which is 24 microns for our conditions. Since η is less than d_p, the Reynolds number is given by

$$Re = \left(\frac{\epsilon d_p^4}{\nu}\right)^{1/3} \tag{14}$$

The Reynolds numbers determined in this way for each particle size were used with the correlation of Brian et al. (1969) to evaluate Sh and k_s. The molecular diffusivity of oxygen in water and the Schmidt number at 25°C used in the calculations are 2.6×10^{-5} cm²/s and 345.

These predicted results for k_s are compared with the experimentally determined values in Table 2. A small error in the measurements used to calculate k_s from k'_{rm} and k'_{rmb} [Equation (9)] leads to a large error in k_s. The agreement between experimental and predicted values is 20% or less. This suggests that the correlations for k_s in the absence of bubbles may be used for a three-phase slurry reactor provided ϵ is corrected for the presence of bubbles. The predicted values for the smaller particle sizes, as given in Table 2, were employed in evaluating $k_r E_f$.

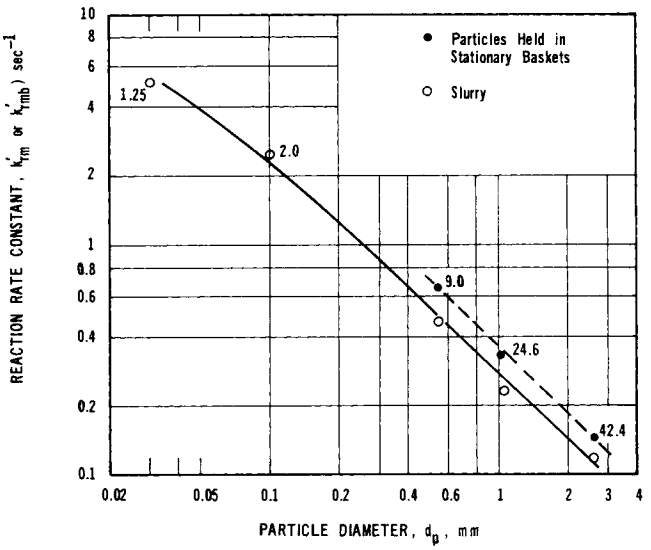

Fig. 2. Dependency of rate constants on particle size (numbers on data points are M_s values).

EFFECTIVENESS FACTORS (E_f) AND INTRINSIC RATE CONSTANT (k_r)

Since $k_s a_s$ and $k_L a_b$ have been obtained, $k_r E_f$ could be determined from Equation (6). Since this subtraction procedure can lead to errors, another method was used in an attempt to reduce such errors. For the two smallest particle sizes, the rate was measured for various M_s and the results shown in Figure 1. According to Equation (5) the slopes of the lines in this figure are equal to $(\rho_p/C^*)(1/k_s a_s + 1/k_r E_f)$. From these slopes and the known values of $k_s a_s$, $k_r E_f$ was determined for these two particles. For the three larger d_p, the results for k'_{rmb} (using baskets) were used in Equation (8) to obtain $k_r E_f$. In these calculations, the value of $k_L a_b V_b$ given by Equation (7) was employed. The so-obtained $k_r E_f$ are listed in Table 2. They vary greatly with particle size showing that intraparticle diffusion significantly affects the reaction rate.

For a first order (in oxygen, see Part I) reaction on a spherical particle the effectiveness factor, effective diffusivity, and intrinsic rate constant are related as follows (Wheeler, 1955):

$$E_f = \frac{3}{M}\left(\coth M - \frac{1}{M}\right) \tag{15}$$

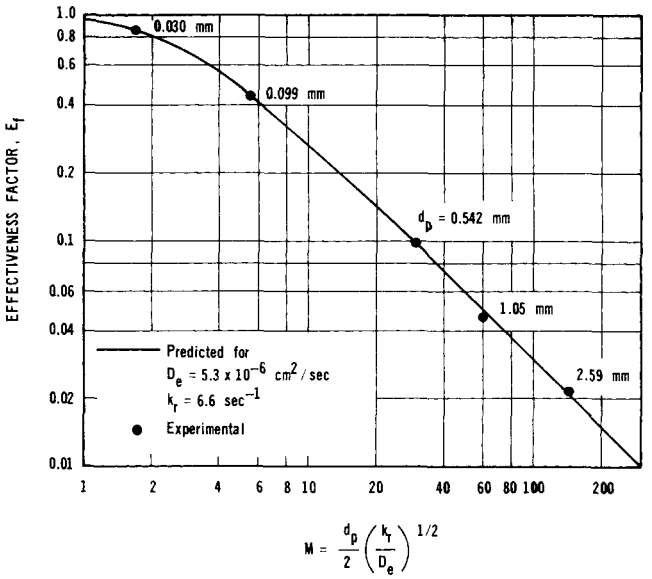

Fig. 3. Effectiveness factors for oxidation of SO_2 in slurries of PAC.

$$M = \frac{d_p}{2}\left(\frac{k_r}{D_e}\right)^{1/2} \tag{16}$$

Equations (15) and (16) along with the data in Table 2 for $k_r E_f$ for various d_p can be solved numerically by trial for k_r and D_e. The results show that the intrinsic rate constant, for the reaction on PAC in water at 25°C, and the effective diffusivity of oxygen in the liquid-filled pores are:

$$k_r = 6.6 \text{ s}^{-1}$$

$$D_e = 5.3 \times 10^{-6} \text{ cm}^2/\text{s}$$

The effectiveness factors labeled experimental in Table 2 were obtained by dividing $k_r E_f$ by k_r. These effectiveness factors agree well (Figure 3) with those calculated from Equations (15) and (16), thus verifying the numerical solution for k_r and D_e. The results show that even for particles as small as 99 microns the effectiveness factor is but 0.45.

The tortuosity factor for oxygen in pores of PAC, as calculated from the expression

$$D_e = \frac{\epsilon_p D}{\tau} \tag{17}$$

was 3.1. This is a reasonable value for pore-volume diffusion alone. In contrast, Furusawa and Smith (1973) showed that the tortuosities for benzaldehyde adsorption, in slurries of PAC in water, were less than unity, suggesting surface diffusion. Also Komiyama and Smith (1974b) found that surface diffusion was important for benzaldehyde in water-filled pores of Amberlite particles. In order to obtain a better understanding of the transport properties involved in the oxidation of SO_2 in aqueous slurries of PAC, adsorption measurements were carried out for H_2SO_4 and SO_2.

INTRAPARTICLE TRANSPORT PROPERTIES FOR H_2SO_4 AND SO_2

Sulfuric Acid

Desorption rates for H_2SO_4 from PAC into water were measured for the 2.59-mm particles. The particles, initially soaked in a 1.92 normal solution of H_2SO_4, were rapidly added to the Pyrex vessel containing well-agitated water (impeller speed = 900 rev./min.). Samples of the slurry liquid were taken at intervals for analysis by titration with 0.01 normal NaOH solution. The run was repeated with the particles held in place by the basket arrangement described previously. As shown in Figure 4, the data for the two runs agreed well with each other, indicating that particle-to-liquid mass transfer resistance was unimportant, in these dynamic experiments, with respect to the resistance for intraparticle diffusion. This may be shown also by noting that the time constant for particle-to-liquid transport is proportional to $1/(k_s a_s)$. Adapting the value of $k_s a_s$ for oxygen from Table 2 to that for H_2SO_4 gives $1/k_s a_s$ of about 1.4 s for the 2.59-mm particles. In contrast, the time required for equalization of the concentration within the pores is proportional to R^2K/D_e. Using the D_e value, determined later (3.20×10^{-6} cm²/s) and the adsorption equilibrium coefficients from Equation (11) of Part I, this time is about 2×10^3 s, a much larger value.

Neglecting particle-to-fluid resistance the conservation equations for sulfuric acid in the slurry liquid and within the particles are

$$V_L \frac{dC_L}{dt} = -D_e\left(\frac{\partial C_r}{\partial r}\right)_{r=R} \tag{18}$$

$$\epsilon_p \frac{\partial C_r}{\partial t} + \rho_p \frac{\partial q}{\partial t} = D_e\left(\frac{\partial^2 C_r}{\partial r^2} + \frac{2}{r}\frac{\partial C_r}{\partial r}\right) \tag{19}$$

With initial and boundary conditions

$$C_L = 0 \quad \text{at} \quad t = 0 \tag{20}$$

$$C_r = \text{constant} \quad \text{at} \quad t = 0 \tag{21}$$

$$\left(\frac{\partial C_r}{\partial r}\right)_{r=0} = 0 \quad \text{at} \quad t \geq 0 \tag{22}$$

$$C_L = (C_r)_{r=R} \quad \text{at} \quad t > 0 \tag{23}$$

It is assumed that the desorption step is rapid with respect to intraparticle diffusion for these relatively large particles. Then the equilibrium relation given by Equation (11) of Part I can be used to relate q and C for H_2SO_4. All the coefficients in Equations (18) to (23) are known except D_e. These equations were solved numerically for $C_L(t)$ for various values of D_e. The results are compared with the experimental data points in Figure 4. The solid curve in the figure for $D_e = 3.2 \times 10^{-6}$ cm²/s fits the data well. The molecular diffusivity of H_2SO_4 in water at 25°C

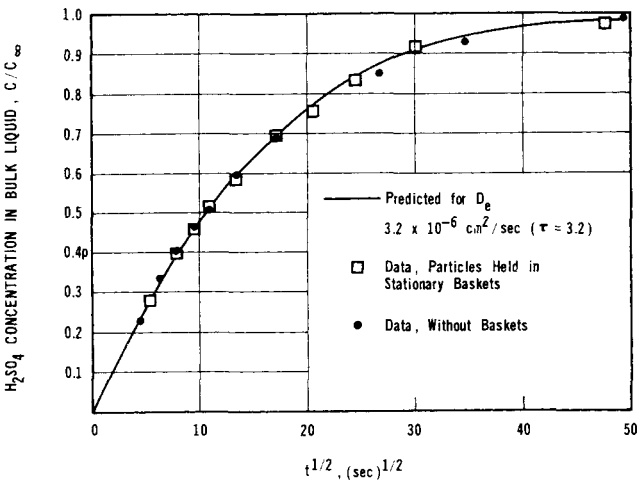

Fig. 4. Desorption curve for sulfuric acid on PAC, 25°C V_L = 1000 cm³, M_s = 17.4 g, $C_{H_2SO_4}$ (in pores, time = 0) = 1.92 normal, d_p = 2.59 mm.

varies from 1.50 to 1.75 $\times$ 10^{-5} cm^2/s with a concentration decrease from 2 to 0.1 normal. At an estimated average concentration of 0.5 normal, $D = 1.62 \times 10^{-5}$ cm^2/s. Then the tortuosity factor calculated from Equation (17) was 3.2. These transport properties for H_2SO_4, as well as the previously established values for oxygen, are given in Table 3. The tortuosity for H_2SO_4 is about the same as that determined for oxygen. When combined with the results given next for SO_2, this suggests that for H_2SO_4 as well as oxygen there is little surface diffusion.

Sulfur Dioxide

Dynamic adsorption runs were made for SO_2 in the same way as described in Part I except that: (1) the larger particles (1.05 and 2.59 mm) were used to increase the intraparticle diffusion resistance, and (2) the particles were placed in the stationary baskets to eliminate the fluid-to-particle resistance. As shown in Part I the bubble-to-liquid resistance was unimportant in the SO_2 experiments. The conservation equations for sulfur dioxide in the slurry liquid and within the particles are:

$$V_L \frac{dC_L}{dt} = F(C_{gi} - C_{go}) - D_e \left(\frac{\partial C_r}{\partial r}\right)_{r=R} \quad (24)$$

$$\epsilon_p \frac{\partial C_r}{\partial t} + \rho_p \frac{\partial q}{\partial t} = D_e \left(\frac{\partial^2 C_r}{\partial r^2} + \frac{2}{r}\frac{\partial C_r}{\partial r}\right) \quad (25)$$

with initial and boundary conditions:

$$C = C_r = 0 \quad \text{at} \quad t = 0 \quad (26)$$

$$\left(\frac{\partial C_r}{\partial r}\right)_{r=0} = 0 \quad \text{at} \quad t \geq 0 \quad (27)$$

$$C_L = (C_r)_{r=R} \quad \text{at} \quad t > 0 \quad (28)$$

The procedure in Part I for evaluating the isotherm for SO_2 showed that the intrinsic adsorption rate at a catalyst site was rapid. Hence, the isotherm given by Equation (10) of Part I can be used for the relation between q and C. Equations (24) to (28) were solved numerically to give $C_L(t)$ for various D_e. A diffusivity of 6.76 $\times$ 10^{-6} cm^2/s results in agreement between predicted curves and the experimental points, as seen in Figure 5. The tortuosity factor calculated from Equation (17), using the available molecular diffusivity for SO_2 in water (Perry, 1963) was 1.6. As summarized in Table 3, this result is significantly smaller than $\tau_{H_2SO_4}$ or τ_{O_2} so that surface transport is indicated for SO_2. In this case the effective diffusivity D_e is given by the sum of pore-volume and surface contribuitons (Komiyama and Smith, 1974b):

$$D_e = \frac{\epsilon_p D}{\tau} + K_f p\, C_{SO_2}{}^{p-1}\, D_s \quad (29)$$

where C_{SO_2} is the SO_2 concentration in the water, K_f and p are the constants in the Freundlich isotherm $q = K_f C^p$ [Equations (10), Part I)], and τ is the tortuosity factor in the pore volume (about 3.2 from the data for H_2SO_4 or O_2). The surface diffusivity calculated from Equation (29) was 2.1 $\times$ 10^{-6} cm^2/s for a C_{SO_2} corresponding to equilibrium with the inlet gas concentration, 2.3% SO_2. Each of the terms in Equation (29) has about the same magnitude so that surface transport appears to be as important as pore-volume transport for SO_2.

DISCUSSION

It is instructive to analyze the relative importance of surface diffusion in terms of the model based upon the binding energy between adsorbate molecules and the surface (Komiyama and Smith, 1974b). This model predicts significant surface transport when the adsorption bond is weak and the adsorption capacity is high. The results in Part I for SO_2 showed that the equilibrium isotherm could be obtained from dynamic experiments and that significant adsorption occurred. These results indicate that weak (physical) adsorption occurred for SO_2. In terms of the model, significant surface diffusion would be expected. In contrast, the capacity for H_2SO_4 adsorption on PAC was low (low values of K and p) so that the surface transport term in Equation (29) is small. The adsorption isotherm for oxygen could not be measured with our methods. However, in Part I the most likely rate determining step for the reaction was found to be the adsorption of oxygen. This suggests that oxygen is chemisorbed on a relatively small number of active sites. The strong chemical interaction with the surface would make the oxygen relatively immobile and explain the observed absence of surface diffusion.

The work reported here indicates that intrinsic activities for the oxidation of SO_2 with activated carbon in slurries can be masked by mass transfer effects, particularly intraparticle diffusion. This can be shown by analyzing the conversion data at room temperature given by Seaburn and Engel (1973) for eight different kinds of carbon particles. A measured rate constant k'_{rm} was calculated first from Equations (12) of Part I and (4) of Part II using the SO_2 conversions, $1 - C_{go}/C_{gi}$, reported by Seaburn and Engel. Then the intrinsic rate constant k_r was estimated in an approximate way by using the following simplifications:

1. In the absence of data, the properties τ, ϵ_p, and ρ_p, and, hence, D_e, were taken to be the same for all the carbons.
2. Bubble-to-liquid and liquid-to-solid mass transfer resistances were neglected.
3. The reaction rate is assumed to be first order in oxygen and zero order for SO_2 as found in Part I for PAC, for all the carbons.

TABLE 3. TRANSPORT PROPERTIES OF PAC (25°C)

	Diffusing substance		
	O_2[a]	H_2SO_4[b]	SO_2[c]
D_e, cm^2/s	5.35 $\times$ 10^{-6}	3.20 $\times$ 10^{-6}	6.76 $\times$ 10^{-6}
D, cm^2/s	2.6 $\times$ 10^{-5}	1.62 $\times$ 10^{-5}	1.7 $\times$ 10^{-5}
τ	3.1	3.2	1.6
D_s, cm^2/s			2.1 $\times$ 10^{-6}

[a] Determined from SO_2 oxidation measurements.
[b] Determined from desorption measurements for H_2SO_4.
[c] Determined from adsorption measurements for SO_2.

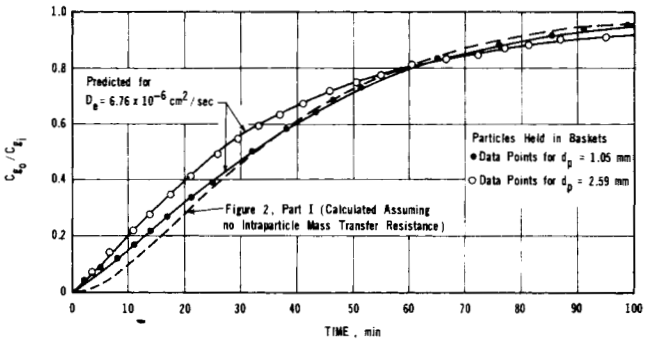

Fig. 5. Dynamic adsorption of SO_2 on PAC, 25°C [V_L = 900 cm^3, M_s = 30 g, C_{g_i} = 2.3%].

Table 4. Estimated Intrinsic Activity of Various Activated Carbon Particles

Carbon type	d_p mm	SO_2 conversion[a] $1 - C_{g0}/C_{gi}$	k'_{rm}, s^{-1}	E_f	k_r, s^{-1}
B.C. YF	0.074	0.75	0.24	1.0	0.24
Norit 14 × 60[c]	0.83	0.67	0.21	0.13	1.6
PAC 12 × 30[c]	1.14	0.6	0.19(0.22)[d]	0.079	2.4(6.6)[e]
Westvaco WV-G	1.05	0.36	0.12	0.16	0.75
NAC G212	1.29	0.30	0.096	0.12	0.80
Witco 12 × 30[c]	1.14	0.27	0.086	0.17	0.51
NAC G107	1.14	0.23	0.074	0.20	0.37
Witco 6 × 12[c]	2.52	0.20	0.064	0.049	1.3

[a] Exp. data from Seaburn and Engel (1973).
[b] Designation according to Seaburn and Engel (1973).
[c] Mesh size range for granular particles.
[d] Evaluated from $k_r = 6.6$ s^{-1} as obtained in present work.
[e] Intrinsic rate constant from present work.

In view of simplification 2, Equation (6) reduces to

$$k'_{rm} = k_r E_f \tag{30}$$

The effectiveness factor for each carbon type was predicted from the known rate, D_e (for oxygen), and particle diameter by expressing Equation (16) in terms of the rate. Eliminating k_r between the last equality in Equation (2) and Equation (16) gives

$$M^2 E_f = \frac{d_p^2}{4D_e}\left(\frac{r_{O_2}\rho_p}{C_s M_s}\right) = \frac{d_p^2}{4D_e}\left(\frac{r_{O_2}\rho_p}{C^* M_s}\right) \tag{31}$$

The surface concentration C_s can be replaced with C^* because of simplification 2. The product $M^2 E_f$ was calculated from Equation (31) and then Equation (15) was used to determine E_f. Finally, k_r was obtained from Equation (30).

In Table 4 the results from Seaburn and Engel (1973) are given in the first three columns where the carbons are listed in decreasing order of the measured conversions of SO_2. The calculated, intrinsic rate constants shown in the last column follow a decidedly different order. The reason for this difference is mostly due to the variation in particle size from carbon to carbon. The effectiveness factor for the Witco 6 × 12 material, which is last in the list, has an effectiveness factor of but 0.049. In terms of intrinsic activity this carbon ranks higher than most of the others.

The value of k'_{rm}, calculated from k_r and D_e measured in this investigation, for 12 × 30 mesh PAC particles, is 0.22 s^{-1}, in good agreement with the value of 0.19 s^{-1} obtained by Seaburn and Engel. The much larger difference between the k_r values (6.6 vs. 2.4 s^{-1}) is due to simplification 2. The effect of this assumption is to reduce the k_r values in Table 4 most for the carbons with a low E_f. Hence, the Witco 6 × 12 particles would have a relatively higher intrinsic rate constant if simplification 2 were not made.

ACKNOWLEDGMENT

The financial assistance of the National Science Foundation for financial support is acknowledged. Also we wish to thank the Pittsburgh Activated Carbon Division of Calgon Corporation for supplying the activated carbon.

NOTATION

C_s = concentration in liquid at surface of particle; C_r = concentration in liquid in pores at radius r, mole/cm³
C_∞ = concentration in liquid at infinite time, mole/cm³
D = molecular diffusivity in liquid, cm²/s
D_e = effective diffusivity, cm²/s
D_s = surface diffusivity, cm²/s
d_b = bubble diameter, cm
d_I = impeller diameter, cm
E_f = catalyst effectiveness factor
K_f = adsorption constant for Freundlich isotherm equation ($q = K_f C^p$)
k'_{rm} = measured reaction rate constant, defined by Equation (4); k'_{rmb} = rate constant measured using baskets, s^{-1}
k_r = intrinsic reaction rate constant, s^{-1}
M = Thiele modulus, defined by Equation (16)
N = impeller speed, rev./s
N_p = power number defined by Equation (11)
P = power consumption of the slurry due to agitation, erg/s
p = exponent of Freundlich isotherm ($q = K_f C^p$)
Re = Reynolds' number defined by Equation (14)
r = radial coordinate in particle (assumed spherical), cm
Sc = Schmidt number (for oxygen-water), ν/D
Sh = $k_s d_p/D$
t = time, s
W = mass of particle-free liquid, g

Greek Letters

ϵ = energy dissipation rate in slurry per unit mass of particle-free liquid, erg/(g)(s)
ϕ = correction factor defined by Equation (12)
ν = kinematic viscosity, cm²/s
τ = tortuosity factor
η = eddy size defined by Equation (13)

LITERATURE CITED

Brian, P. L. T., H. B. Hales, and T. K. Sherwood, "Transport of Heat and Mass Between Liquid and Spherical Particles in an Agitated Tank," *AIChE J.*, **15**, 727 (1969).

Calderbank, P. H., "Physical Rate Processes in Industrial Fermentation," *Trans. Inst. Chem. Engrs.*, Part I, **36**, 443 (1958); Part II **37**, 173 (1959).

Furusawa, T., and J. M. Smith, "Fluid-Particle and Intraparticle Mass Transport Rates in Slurries," *Ind. Eng. Chem. Fundamentals*, **12**, 197 (1973).

Juvekar, V. A., and M. M. Sharma, "Adsorption of CO_2 in a Suspension of Lime," *Chem. Eng. Sci.*, **28**, 825 (1973).

Komiyama, H., and J. M. Smith, "Intraparticle Mass Transport in Liquid-Filled Pores," *AIChE J.*, **20**, 728 (1974).

———., "Surface Diffusion in Liquid-Filled Pores," *AIChE J.*, **20**, 1110 (1974).

Levins, D. M., and J. R. Glastonburg, "Particle-Liquid Hydrodynamics and Mass Transfer in a Stirred Vessel," *Trans. Inst. Chem. Engrs.*, **50**, 132 (1972).

Loomis, A. G., *International Critical Tables*, **3**, 257 (1929).

Misic, D. M., and J. M. Smith, "Adsorption of Benzene in Carbon Slurries," *Ind. Eng. Chem. Fundamentals*, **10**, 380 (1971).

Perry, J. H., *Chemical Engineer's Handbook*, 4 ed., p. 14, McGraw-Hill, New York (1963).

Prasher, B. D., and G. B. Wills, "Mass Transfer in an Agitated Vessel," *Ind. Eng. Chem. Process Design Develop.*, **12**, 351 (1973).

Seaburn, J. T., and A. J. Engel, "Sorption of Sulfur Dioxide by Suspension of Activated Carbon in Water," *AIChE Symp. Ser. No. 134*, **69**, 71 (1973).

Sherwood, T. K., and E. J. Farkas, "Studies of the Slurry Reactor," *Chem. Eng. Sci.*, **21**, 573 (1966).

Wheeler, A., "Catalysis," Vol. II, 105, Reinhold, New York (1955).

Manuscript received October 23, 1974; revision received and accepted January 24, 1975.